Amino Acids (2010) 38:319–327
DOI 10.1007/s00726-009-0253-8

ORIGINAL ARTICLE

Quantum chemical investigation of nitrotyrosine (3-nitro-L-tyrosine) and 8-nitroguanine

Şakir Erkoç · Figen Erkoç · Aylin Sepici-Dinçel

Received: 22 December 2008 / Accepted: 2 February 2009 / Published online: 19 February 2009

Abstract The structural, vibrational and electronic properties of nitrotyrosine and 8-nitroguanine have been investigated theoretically by performing the molecular mechanics (MM+ force field), the semi-empirical self-consistent-field molecular-orbital (PM3), and density functional theory calculations. The geometry of the nitrotyrosine and 8-nitroguanine molecules have been optimized, the vibrational dynamics and the electronic properties calculated in their ground states in the gas phase.

Keywords Nitrotyrosine · 8-Nitroguanine · Semiempirical calculations · Ab initio calculations · Density functional calculations

Introduction

The nitration of protein tyrosine residues, both in protein-bound form and free amino acid form, constitutes the substitution of hydrogen by a nitro group at the 3-position of the phenolic ring where the initial reaction is the oxidation of the aromatic ring of tyrosine and then represents a post-translational modification produced by nitric oxide derived oxidants such as peroxynitrite ($ONOO^-$) and nitrogen dioxide radical (additional step). The principal difference between both reaction pathways lies in the oxidation step that generates $Tyr^{\cdot}$ by a one-electron oxidation process (Radi 2004; Peluffo and Radi 2007). The increase of 3-nitrotyrosine (NOTYR; CAS: 621-44-3, MW: 226.19) to levels well above basal levels is established to serve as a footprint of nitro-oxidative damage in vivo both in animal models and human diseases and can be used as a strong biomarker (Bartesaghi et al. 2007).

Nitration of protein tyrosine residues in vivo is widely used as a bioassay indicative of $ONOO^-$ generation. Peroxynitrite added to cells, tissues, and body fluids leads to important biological processes such as:

1. Rapid protonation.
2. Followed by $ONOOH^-$ dependent depletion of −SH groups and other antioxidants. Among protein targets of attack are glutathione transferases, manganese superoxide dismutase, structural proteins such as actin and neurofilament L and α-synuclein, prostacyclin synthase, ribonucleotide reductase, the copper transport protein cerruloplasmin, and sarcoplasmic reticulum Ca^{2+}-ATPase.
3. Oxidaiton of lipids.
4. DNA strand breakage.
5. Nitration and deamination of DNA bases (especially guanine).
6. Nitration of aromatic amino acid residues in proteins. The most studied reaction in proteins has been conversion of tyrosine to 3-nitrotyrosine, but tryptophan and phenylalanine can also be nitrated.
7. Methionine oxidation to its sulphoxide.
8. Addition of $ONOO^-$ (like that of HOCl) causes inactivation of α_1-antiproteinase.

Ş. Erkoç (✉)
Department of Physics, Middle East Technical University, 06531 Ankara, Turkey
e-mail: erkoc@metu.edu.tr

F. Erkoç
Department of Biology Education, Gazi University, 06500 Ankara, Turkey

A. Sepici-Dinçel
Department of Medical Biochemistry, Faculty of Medicine, Gazi University, Ankara, Turkey

Levels of protein 3-nitrotyrosine in stressed tissues are in the range of 10–100 pmol/mg, corresponding to about 1–5 nitrated residues over 10,000 tyrosines (100–500 μmol/mol). Mitochondrial proteins are also important targets for reactive oxygen and nitrogen species. A wide spectrum of other peroxidase-like hemoproteins such as cytochrome *c*, present in diverse cell types, is capable of catalyzing tyrosine nitration. Nitrotyrosine is a relatively large and bulky amino acid, and tyrosine nitration may greatly change the chemical and biological properties of soluble tyrosine and tyrosine-containing proteins leading to altered protein conformation, solubility, susceptibility to aggregation and increased protein degradation (Chou 1988, 2004).

Nitric oxide radical ($NO^{\cdot}$) synthesized by tissues such as the vascular endothelial cells reacts rapidly with superoxide anion giving peroxynitrite (1), peroxyl radicals to giving alkyl peroxynitrite (2), and hydroxyl radical giving nitrous acid (3) which are reactive nitrogen species (RNS):

$$O_2^- + NO^{\cdot} \rightarrow ONOO^- \quad (1)$$

$$RO_2^{\cdot} + NO^{\cdot} \rightarrow ROONO \quad (2)$$

$$NO^{\cdot} + OH^{\cdot} \rightarrow HNO_2 \quad (3)$$

Similar to attack of tyrosine residues in proteins by RNS, HOCl also attacks tyrosine leading to chlorination. Nitrotyrosines, have been detected in various inflammatory processes including atherosclerotic lesions/plaques, cardiac disease (both Apo A and to a lesser extent Apo B are nitrated in vitro and in vivo and apolipoprotein nitration increases in cardiovascular patients), rheumatoid arthritis, multiple sclerosis, cystic fibrosis, Alzheimer's disease, chronic renal failure and septic shock. Nitrotyrosine levels have been detected in human plasma and urine; concentrations are higher in body fluids/tissues from patients with chronic inflammatory diseases. Elevated levels of NOTYR have been shown to cause DNA damage or trigger apoptosis and can be also observed in rejected kidney transplants. It is also used as predictor of disease progression and severity in conditions such as acute and chronic inflammatory processes, cardiovascular disease, neurodegeneration and diabetic complications. Upregulation of the inducible isoform of nitric oxide synthase (iNOS) has been shown to accompany inflammation in certain tissues (Bartesaghi et al. 2007; Halliwell and Gutteridge 2001; Castro et al. 2004).

Another interesting application of NOTYR is use as a spectroscopic probe in the study of protein–protein interactions as an alternative to tryptophan and fluorescence resonance energy transfer (FRET) studies, since it has great potential as an energy acceptor in FRET and, indeed, direct chemical nitration of tyrosine was used to investigate the structural and folding properties of certain proteins such as calmodulin and apomyoglobin (De Fillipis et al. 2006).

Nitration and deamination of DNA bases (especially guanine at C8) by RNS ($^{\cdot}NO_2$, ONOOH, N_2O_3, HNO_2) can produce nitration, nitrosation and deamination of DNA bases such as 8-nitroguanine and deamination products xanthine and hypoxanthine. 8-Nitroguanine (NTRGU) rapidly depurinates from DNA (base abstraction, abasic site, leading to potential mutagenesis), forming an apurinic site in the DNA in vitro (Yermilov et al. 1995a) and therefore has been considered as a marker for nitrative nucleic acid damage. Additionally G:C to T:A transversions were shown experimentally. Yermilov et al. (1995b) were the first researchers to show guanine rapidly reacting with the strong oxidant peroxynitrite anion to form NTRGU; nitration of tyrosine did not lead to nitration of guanine. Later 8-oxoguanine was also shown as a target for nitration (Niles et al. 2006; Kawanishi et al. 2006). Akuta et al. (2006) identified biologically formed NTRGU as a potential biomarker and contributor for nitrative stress occurring during infections and inflammation and NTRGU was also found, along with 8-oxodeoxyguanosine, in gastric gland epithelial cells in patients and mice infected with *Helicobacter pylori* (Akuta et al. 2006). Nitrative stress via guanine nitration is presently a critical area of research not only in pathogenesis but also in molecular mechanisms of the pathogenesis of many diseases (Sawa and Ohshima 2006).

Free as well as esterified fatty acids are important components of lipoproteins and membranes that can be modified by oxidative and nitrative damage and their reactivity determined by the biological environment of target molecules. Current data reveal that nitrated fatty acids also serve as mediators of physiological and pathophysiological cell signaling processes, including vascular cell and inflammatory signaling (Trostchansky and Rubbo 2008). Sulfation of nitrotyrosine, by cytosolic sulfotransferases, as a possible means for the detoxification and/or disposal of free nitrotyrosine by cells in vivo has been reviewed by Liu et al. (2007).

Dong et al. (2007) studied the less well known interactions of NOTYR with reactive oxygen species (ROSs). Oxidation behavior of NOTYR by hydroxyl radical generation after gamma irradiation was chosen as the model for ROSs. Density functional theory (DFT) calculation was employed to investigate the reactivity of nitrotyrosine with hydroxyl radical. They concluded that gamma radiation-induced hydroxylation with hydroxyl radicals was selectively at C5 (C5 of (Dong et al. 2007) corresponds to C2 in the present study) of the benzene ring, producing 3,4-dihydroxy-5-nitrophenylalanine from NOTYR (Dong et al. 2007).

The reaction of NO with tyrosyl radical has been proposed as a mechanism of action for interference of NO with the catalytic activities of certain enzymes via tyrosine iminoxyl radical (Scheme 1 of Gunther et al. 2002). The determination of the origin of nitrotyrosine in vivo is a difficult problem; at least six distinct biochemical pathways to nitrotyrosine have been proposed, all of which require nitric oxide (or its products) and ROS (Gunther et al. 2002). Recently DFT, calculations were carried out at the B3LYP/cc-pVTZ level of theory to obtain a complete investigation of the interactions between $Tyr^{\cdot}$ and $NO^{\cdot}$ by using theoretical methods for exploring in detail the Tyr-NO_2 formation mechanism (Fig. 3 of Papavasileiou et al. 2007). They also concluded that the reaction proceeds via an iminoxyl radical.

Sadeghipour et al. (2005) studied the ability of 11 flavonoids (naturally occurring polyphenols) and their related structure–activity relationships (SARs) for inhibiting peroxynitrite-induced nitration of tyrosine and hence protection of cells from potential toxic effects by using molecular modeling with theoretical approaches. They performed geometry optimizations by applying semi-empirical method PM3 and obtained SAR data by applying single-point calculations at the DFT/B3LYP level (Sadeghipour et al. 2005).

The aim of the present theoretical study is to investigate the structural, electronic and vibrational properties of nitrotyrosine (NOTYR) and 8-nitroguanine (NTRGU) due to the potential biological and medical significance of protein tyrosine nitration and DNA damage via nucleobases such as guanine. There are limited studies in the literature about the molecules considered in this work. The results of such theoretical work will aid in the elucidation of SARs and mechanisms of action of NOTYR, NTRGU and similar biologically reactive intermediates, since evaluation of new activities or interactions by nitrated proteins and damaged DNA becomes a relevant matter in the context of alterations of cell homeostasis by nitro-oxidative stress. Work on the development of NTRGU as a promising biomarker to evaluate the potential risk of inflammation-mediated carcinogenesis still continues. The species causing tyrosine nitration usually have very short half-lives, and measuring them directly in the biological system is extremely difficult; therefore, theoretical methods are preferred to investigate these systems at the atomic and molecular levels.

Computational methods

The geometries of nitrotyrosine (NOTYR) and 8-nitroguanine (NTRGU) have been optimized using different levels of quantum chemical calculations. Preoptimizations have been performed by applying the molecular mechanics (MM) method (Burkert and Allinger 1982) using MM+ force field (Allinger 1977). The high computational speed of molecular mechanics makes it easier to perform better optimization using a higher level of computation methods. These optimized structures were taken and the semi-empirical self-consistent-field molecular-orbital (SCF-MO) method (Stewart 1990) at PM3 (Stewart 1989) level within the restricted Hartree-Fock (RHF) formalism (Roothaan 1951) have been applied to fully optimize the structures and calculate the vibrational spectra. Geometry optimizations are carried out by using a conjugate gradient method (Polak-Ribiere algorithm) (Fletcher 2000). The RMS gradient of 10^{-5} was set to get sufficient structural optimization. Harmonic frequency analysis indicated that all stationary points were found to be true minima (there was no imaginary frequency). At the end, the geometry taken from PM3 was used to perform single-point calculations with DFT (Kohn and Sham 1965) using Becke's three-parameter exchange functional (Becke 1993) with the Lee–Yang–Parr correlation functional (Lee et al. 1988) (B3LYP). Density functional theory calculations have been realized using the 6-31G* basis set (Hehre et al. 1972). All these calculations have been carried out with HyperChem 7.5 program package (Hypercube Inc. 2002).

Results

Optimized structures

Preoptimization by the MM method using MM+ force field is quite fast and gives a reliable optimized structure. In the second stage of the optimization procedure the PM3 method has been applied by taking care of relatively fine criteria. Figure 1 shows the final form of the optimized structure (in ball and stick models) of NOTYR and NTRGU. Figure 2 displays the atom symbols and labels in stick models. The bond-lengths are displayed in Fig. 3. After MM optimization, energy contributions are given in Table 1. As seen from Table 1, the dominant positive contribution to total energy of NOTYR comes from Vdw interactions, whereas the dominant negative contributions come both from dihedral and electrostatic interactions. The resultant total energy has a negative value. On the other hand, the dominant positive contribution to total energy of NTRGU comes from angle bending, whereas the dominant negative contribution comes from electrostatic interactions. The resultant total energy has a positive energy. The characteristics (magnitude and sign) of MM energy contributions are quite different in these two molecules. After the PM3 optimization some of the calculated energy values are given in Table 2. According to the PM3 calculation the

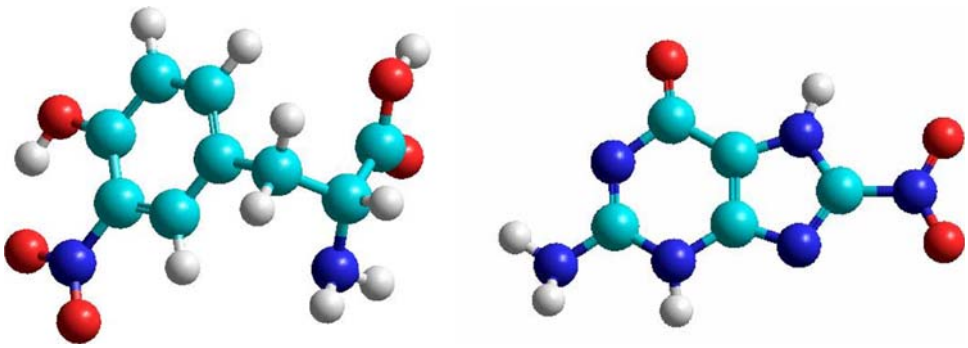

Fig. 1 Ball and stick models of the optimized structures of NOTYR (*left*) and NTRGU (*right*) molecules (PM3 results)

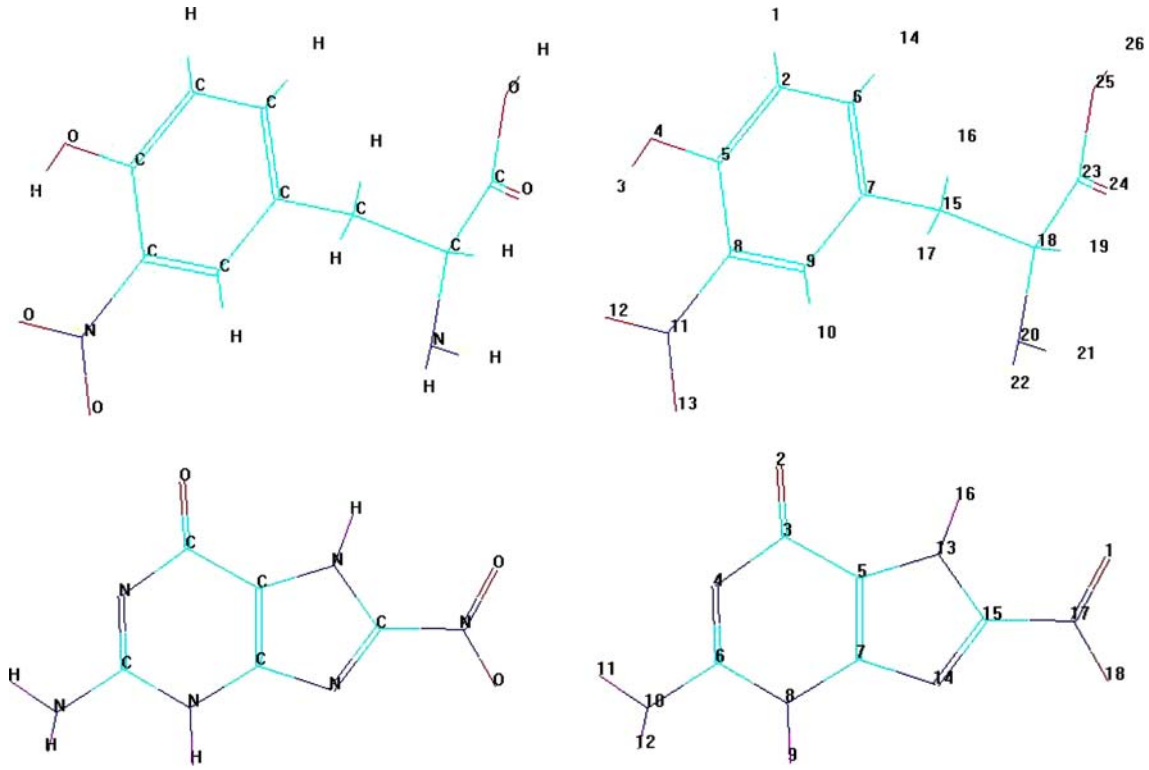

Fig. 2 Stick models of the optimized structures of NOTYR (*upper*) and NTRGU (*lower*) molecules (PM3 results)

heat of formation of NOTYR is exothermic and has the value of ca. −125 kcal/mol, whereas it is endothermic for NTRGU and has the value of ca. 4 kcal/mol.

Vibrational analysis

The vibrational spectra of NOTYR and NTRGU, namely, the infrared spectrum (IRS) (in harmonic approximation) have been calculated within the PM3 level. The IRS, including both frequencies and the corresponding intensities, are shown in Fig. 4. There are 72 and 42 normal modes (harmonic vibrations) for the molecules studied NOTYR and NTRGU, respectively. The first eight modes with relatively largest intensity are given in Table 3. In the case of NOTYR molecule, the vibrations with the first two largest intensities are due to the twisting of the bond C8–N11. The vibration with the third largest intensity is due to the twisting of the bond C18–C23. The vibration with the fourth largest intensity is due to the shrinking and expansion of the benzene ring along C5–C7 direction and the stretching of the bonds O6–C5 and N11–C8. The vibration with the fifth largest intensity is due to the twisting of the bond O4–C5. The calculated IRS qualitatively agrees with experimentally determined FTIR spectrum (URL1 2008). The FTIR spectrum of NOTYR features three main bands; the first band contains a series of peaks between 450 and 900 cm^{-1}, the second band contains a series of peaks between 1,000 and 1,700 cm^{-1}, and the third band contains a series of peaks between 2,800 and 3,300 cm^{-1}. The intensities of the peaks in the first band

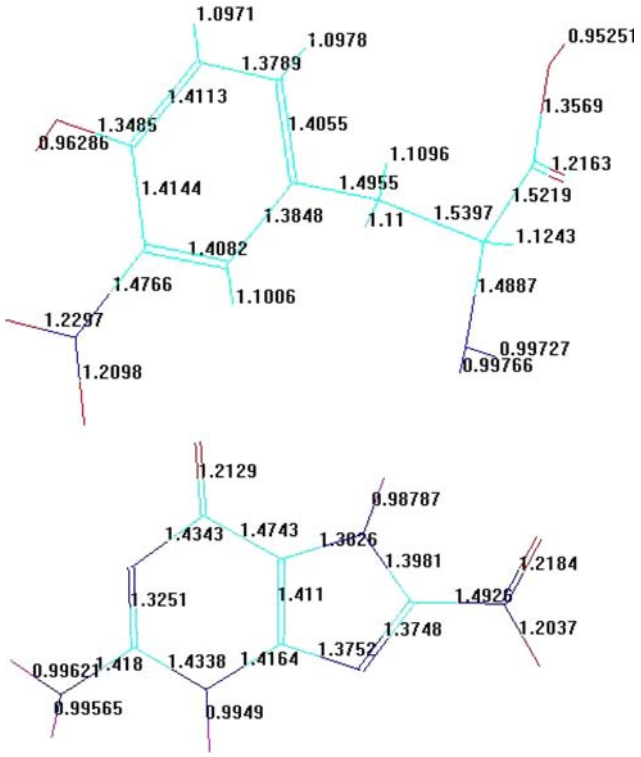

Fig. 3 Bond-lengths of the optimized structures of NOTYR (*upper*) and NTRGU (*lower*) molecules (PM3 results)

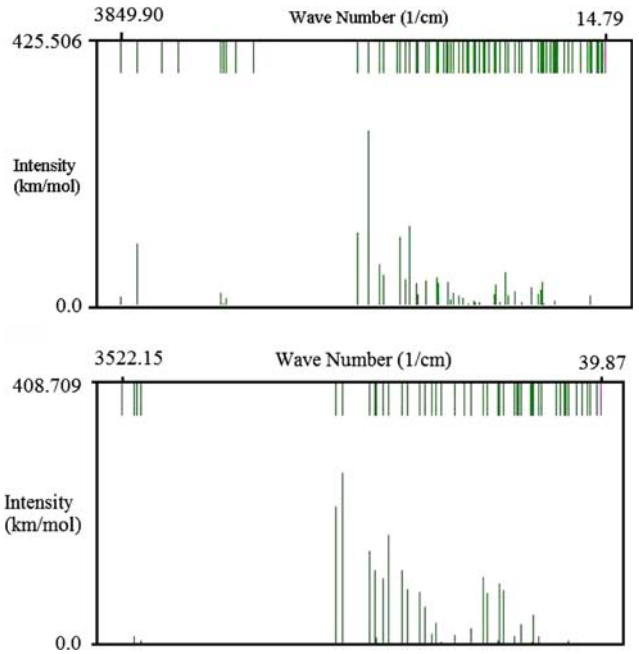

Fig. 4 Calculated infrared spectra of NOTYR (*upper*) and NTRGU (*lower*) molecules (PM3 results)

Table 1 Energy contributions (in kcal/mol) after MM method with MM+ force field

Contribution	NOTYR	NTRGU
Bond	0.460884	0.69176
Angle	1.51389	17.3064
Dihedral	−6.10937	4.47
Vdw	7.25102	2.69
Stretch-bend	0.0409798	−0.424015
Electrostatic	−5.01583	−14.9259
Total	−1.858416	9.808238

Table 2 Calculated energies (in kcal/mol) after PM3 method

Quantity	NOTYR	NTRGU
Total energy	−69439.838	−57772.834
Binding energy	−2707.346	−1915.587
Isolated atomic energy	−66732.492	−55857.247
Electronic energy	−399455.046	−302363.246
Core-core interaction	330015.208	244590.412
Heat of formation	−124.521	3.948

Table 3 The first eight relatively largest infrared intensities (in km/mol) and the corresponding harmonic frequencies (in cm^{-1}) after PM3 method

NOTYR		NTRGU	
Intensity	Frequency	Intensity	Frequency
283.671	1887.01	272.473	1923.53
131.182	1565.85	219.787	1965.20
118.442	1978.55	175.974	1579.20
113.304	1641.06	150.399	1721.49
102.710	3725.39	121.960	1480.72
69.274	1803.36	120.960	1685.81
56.574	807.83	111.052	898.13
51.013	1766.33	107.512	1624.01

are relatively smaller than the other peaks taking place in the second and third bands. On the other hand, in the case of the NTRGU molecule, the vibrations with the first and the third largest intensities are due to the twisting of the bond C15–N17. The vibration with the second largest intensity is due to the bond stretching of the bond C3–O2. The fourth largest intensity is due to the vibration of bond stretching of the bond C5–C7. To the knowledge of the authors, there is no available experimental spectrum in the literature for the NTRGU molecule. The PM3 harmonic frequencies should be scaled by 0.976 to compare experimental values (Scott and Radom 1996).

Electronic properties

Electronic properties have been obtained by performing the DFT/B3LYP/6-31G* level calculation. Some of the

Table 4 Some of the calculated quantities after DFT method

Quantity	NOTYR	NTRGU
Total energy (kcal/mol)	−523380.916	−468519.665
Electronic kinetic energy (kcal/mol)	519023.447	464247.897
eK, ee and eN energy (kcal/mol)	−1217656.454	−1005371.153
Nuclear repulsion energy (kcal/mol)	694275.538	536851.488
Lowest MO (eV)	−522.370	−522.404
LUMO (eV)	−6.353	−6.899
HOMO (eV)	−2.253	−2.872
Highest MO (eV)	131.067	129.873
HOMO–LUMO difference, E_g (eV)	4.10	4.03
Dipole moment, μ (Debye)	5.2871	5.3784
Virial ($-V/T$)	2.0084	2.0092

calculated energy values are given in Table 4. Molecular orbital eigenvalue spectra of the molecules studied are shown in Fig. 5. The 3D pictures of the highest occupied molecular orbital (HOMO) and the lowest unoccupied molecular orbital (LUMO) are displayed in Fig. 6. As seen from Fig. 6, in the case of the NOTYR molecule, HOMO is localized mainly on the benzene ring, whereas LUMO is localized mainly on the NO_2 branch. The location of LUMO may be interpreted as NOTYR may form radical on the NO_2 branch. On the other hand, in the case of the NTRGU molecule, HOMO is mainly localized on the C5–C7 double bond, and LUMO is mainly localized on the C15–N17 bond and the oxygens O1 and O18. The location of LUMO in the NTRGU molecule may be interpreted as, similar to NOTYR molecule, NTRGU may form radical on the NOO functional group. HOMO–LUMO energy difference, E_g, of both NOTYR and NTRGU are close to each other, they have been calculated to be ca. 4.1 and 4.0 eV, respectively.

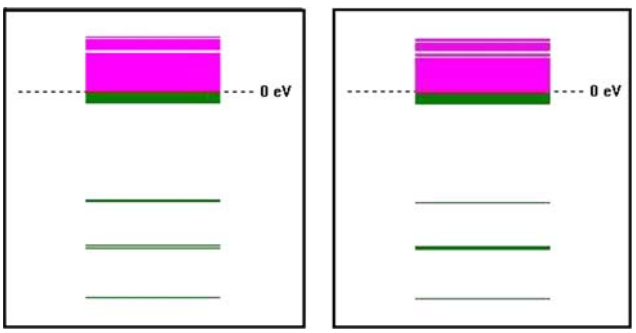

Fig. 5 Molecular orbital eigenvalue spectra of NOTYR (*left*) and NTRGU (*right*) molecules (DFT results). Lowest and highest MO values are given in Table 4

The calculated dipole moment of both NOTYR and NTRGU are close to each other, they are about 5.3 and 5.4 D (Debyes), respectively. Comparing this value to that of water (exp. 1.85 D, same level of cal. 2.02 D), both NOTYR and NTRGU have large dipole moments, and seem to be polar (hydrophilic). The excess charge on atoms is displayed in Fig. 7.

Discussion

Biologically critical molecules in the cell such as DNA and protein are under potential oxidative/nitrative stress and cell homeostasis can be established depending on the defense systems status. Overall, in solutions buffered at physiologic pH and containing CO_2, the major reactive species are expected to be CO_3^{-}, $^{\cdot}NO_2$, and $ONOO^{-}$, along with minor amounts of ONOOH and $HO^{\cdot}$. These reactive intermediates lead to the formation of a spectrum of oxidation products, later nitration reactions initiated with $ONOO^{-}$. The resulting ROS and RNS are of importance when cell and tissue level damage and toxic effects are considered. DNA base modifications induced by RNS can occur by four types of chemical reaction: (i) alkylation via nitrosamine formation, (ii) deamination, (iii) oxidation, and (iv) nitration. Both molecules studied have nitration potential together with similar hydrogen bonding groups and therefore may pose a risk to cells and their aqueous environment (De Fillips et al. 2006; Fletcher 2000). However, both molecules have also been considered as biomarkers for the assessment of nitrative stress in a number of disease states.

The structural, vibrational and electronic properties of the molecules studied are given in detail in the section "Results". The bond length C15–C18 is the largest bond in the molecule NOTYR and may fragment easily by breaking of this bond. On the other hand, the bond length C15–N17 is the largest bond in the molecule NTRGU. This information may indicate that NTRGU is relatively more stable than NOTYR in gas phase. Also HOMO–LUMO energy difference, E_g, of both NOTYR and NTRGU are close to each other. That value of E_g may be considered as relatively small and indicates that both NOTYR and NTRGU molecules have low kinetic lability. The calculated excess charge on atoms shows an interesting feature. For instance, in the case of the NOTYR molecule, the nitrogen atom bonded to benzene ring (N11) has a positive excess charge of ca. +0.4e, whereas the other nitrogen atom (N20) has a negative excess charge of ca. −0.7e. This feature of excess charge on atoms may play an important role in the interaction of NOTYR with its environment. The positively charged nitrogen atom (N11) forms a negative terminal due to the negatively charged oxygen atoms (O12, O13), which may be attracted to its environment. Similarly the O24 is

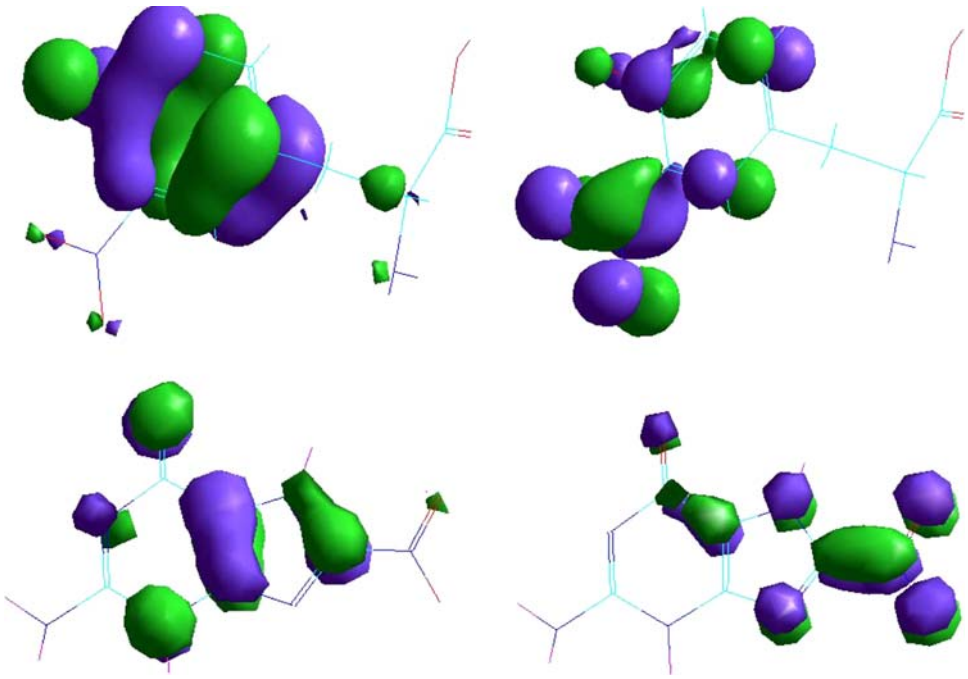

Fig. 6 HOMO (*left*) and LUMO (*right*) of NOTYR (*upper*) and NTRGU (*lower*) molecules (DFT results)

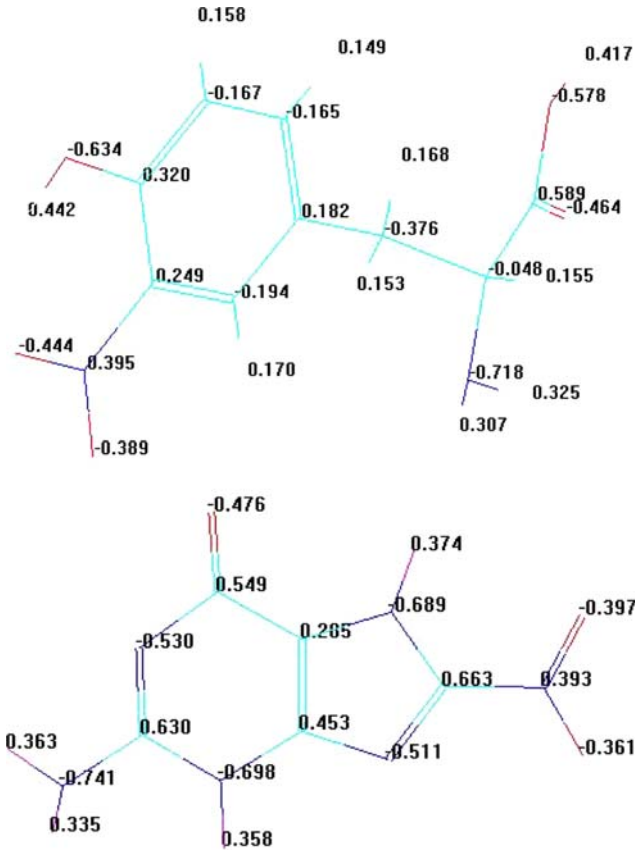

Fig. 7 Excess charge on atoms of NOTYR (*upper*) and NTRGU (*lower*) molecules (DFT results)

also an attractive terminal for its environment. On the other hand, in the case of the NTRGU molecule, all the nitrogen atoms, except N17, have negative charge accumulation, N17 has positive charge accumulation. The NOO functional group of NTRGU has similar characteristics to that of the NOTYR molecule. Figure 8 shows the 3D pictures of the charge density and the electrostatic potential. In the case of the NOTYR molecule, the negatively charged nitrogen atom (N20) forms a positive terminal due to the positively charged hydrogen atoms (H21, H22), which may be attracted to water molecules. Similarly the H3 and H26 atoms are also positively charged, which are also attracted to water molecules. Water molecules can be bonded to positively charged hydrogens through hydrogen bonding type interaction. Moreover, the NH_2 terminal interacts first when a molecule (a radical) approaches NOTYR; furthermore, this part of NOTYR may react with phosphate groups of DNA. Similar features are also valid for the NTRGU molecule. The present calculation results for NTRGU show similar features to that of guanine and guanosine (Erkoç and Erkoç 2002). Furthermore, Liu et al. (2006) investigated reaction mechanisms of peroxynitrite oxidation of guanine considering the same level of calculation as done in the present study. The features of NTRGU seen in this work also agree with those of Liu et al. (2006).

The results of the present study may be employed in the development and further studies of the molecules as

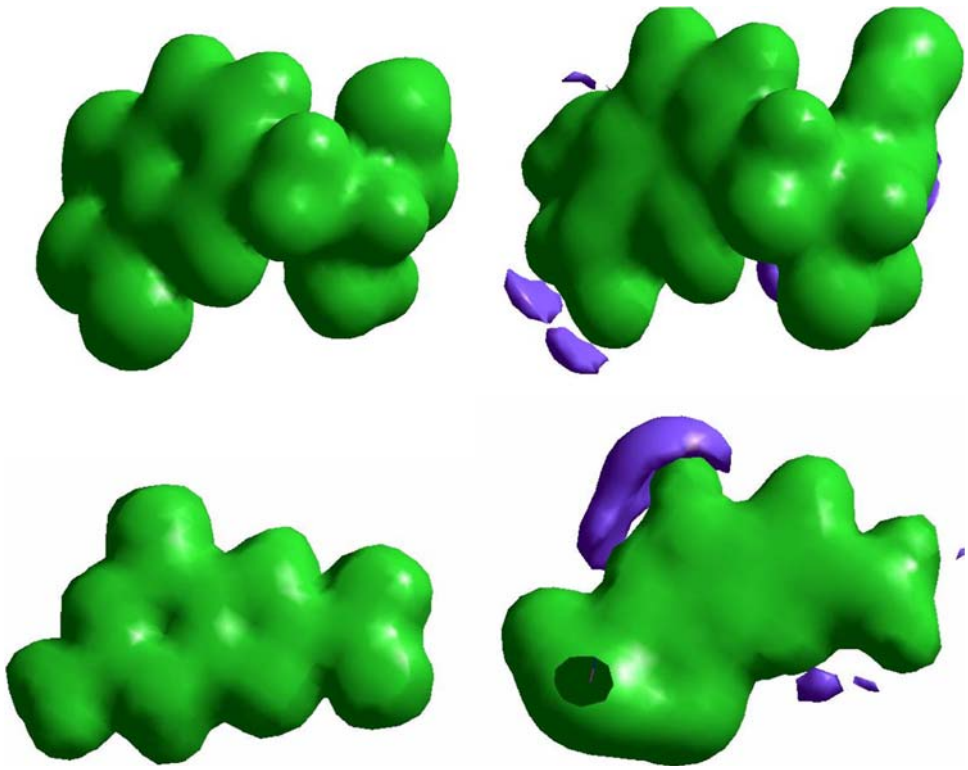

Fig. 8 Charge density (*left*) and electrostatic potential (*right*) of NOTYR (*upper*) and NTRGU (*lower*) molecules (DFT results)

biomarkers for inflammatory situations and also inflammation-mediated carcinogenesis. Efforts for using NTRGU in urine released from DNA damage are available. However, NTRGU from tissue RNA is still to be considered as a biomarker since it is more stable than the DNA products.

Acknowledgment The author (SE) would like to thank METU for partial support through the project METU-BAP-08-11-DPT-2002-K120-510.

References

Akuta T, Zaki MH, Yoshitake J, Okamoto T, Akaike T (2006) Nitrative stress through formation of 8-nitroguanosine: insights into microbial pathogenesis. Nitric Oxide 14:101–108. doi:10.1016/j.niox.2005.10.004

Allinger NL (1977) Conformational analysis 130. MM2. A hydrocarbon force field utilizing V_1 and V_2 torsional terms. J Am Chem Soc 99:8127–8134. doi:10.1021/ja00467a001

Bartesaghi S, Ferrer-Sueta G, Peluffo G, Valez V, Zhang H, Kalyanaraman B, Radi R (2007) Protein tyrosine nitration in hydrophilic and hydrophobic environments. Amino Acids 32:501–515. doi:10.1007/s00726-006-0425-8

Becke AD (1993) Density-functional thermochemistry. III. The role of exact exchange. J Chem Phys 98:5648–5652. doi:10.1063/1.464913

Burkert U, Allinger NL (1982) Molecular mechanics. ACS Monograph, vol 177, Washington

Castro L, Eiserich JP, Sweeney S, Radi R, Freeman BA (2004) Cytochrome *c*: a catalyst and target of nitrite-hydrogen peroxide-dependent protein nitration. Arch Biochem Biophys 421:99–107. doi:10.1016/j.abb.2003.08.033

Chou KC (1988) Low-frequency collective motion in biomacromolecules and its biological functions. Biophys Chem 30:3–48. doi:10.1016/0301-4622(88)85002-6

Chou KC (2004) Structural bioinformatics and its impact to biomedical science. Curr Biomed Chem 11:2105–2134

De Fillipis V, Frasson R, Fontana A (2006) 3-Nitrotyrosine as a spectroscopic probe for investigating protein–protein interactions. Protein Sci 15:976–986. doi:10.1110/ps.051957006

Dong JC, Shi WQ, Zhao YF, Li YM (2007) Hydroxylation of 3-nitrotyrosine by hydroxyl radical. Chin Chem Lett 18:542–544. doi:10.1016/j.cclet.2007.03.032

Erkoç F, Erkoç Ş (2002) Structural and electronic properties of guanine and guanosine. J Mol Struct Theochem 589–590:405–411. doi:10.1016/S0166-1280(02)00298-1

Fletcher P (2000) Practical methods of optimization. Wiley-VCH, Weinheim

Gunther MR, Sturgeon BE, Mason RP (2002) Nitric oxide trapping of the tyrosyl radical-chemistry and biochemistry. Toxicology 177:1–9. doi:10.1016/S0300-483X(02)00191-9

Halliwell B, Gutteridge JMC (2001) Free radicals in biology and medicine, 3rd edn. Oxford University Press, Oxford

Hehre WJ, Ditchfield R, Pople JA (1972) Self-consistent molecular orbital methods. XII. Further extensions of gaussian-type basis sets for use in molecular orbital studies of organic molecules. J Chem Phys 56:2257–2261. doi:10.1063/1.1677527

Hypercube, Inc. (2002) Gainesville, FL, USA

Kawanishi S, Hiraku Y, Pinlaor S, Ma N (2006) Oxidative and nitrative DNA damage in animals and patients with inflammatory diseases in relation to inflammation-related carcinogenesis. Biol Chem 387:365–372. doi:10.1515/BC.2006.049

Kohn W, Sham LJ (1965) Self-consistent equations including exchange and correlation effects. Phys Rev 140:A1133–A1138. doi:10.1103/PhysRev.140.A1133

Lee C, Yang W, Parr RG (1988) Development of the Colle-Salvetti correlation-energy formula into a functional of the electron density. Phys Rev B 37:785–789. doi:10.1103/PhysRevB.37.785

Liu N, Ban F, Boyd RJ (2006) Modeling competitive reaction mechanisms of peroxynitrite oxidation of guanine. J Phys Chem A 110:9908–9914. doi:10.1021/jp061297b

Liu MC, Yasuda S, Idell S (2007) Sulfation of nitrotyrosine: biochemistry and functional implications. IUBMB Life 59:622–627. doi:10.1080/15216540701589320

Niles JC, Wishnok JS, Tannenbaum SR (2006) Peroxynitrite-induced oxidation and nitration products of guanine and 8-oxoguanine: structures and mechanisms of product formation. Nitric Oxide 14:109–121. doi:10.1016/j.niox.2005.11.001

Papavasileiou KD, Tzima TD, Sanakis Y, Melissas VS (2007) A DFT study of the nitric oxide and tyrosyl radical interaction: a proposed radical mechanism. Chem Phys Chem 8:2595–2602. doi:10.1002/cphc.200700434

Peluffo G, Radi R (2007) Biochemistry of protein tyrosine nitration in cardiovascular pathology. Cardiovasc Res 75:291–302. doi:10.1016/j.cardiores.2007.04.024

Radi R (2004) Nitric oxide, oxidants, and protein tyrosine nitration. Proc Natl Acad Sci USA 101:4003–4008. doi:10.1073/pnas.0307446101

Roothaan CC (1951) New developments in molecular orbital theory. Rev Mod Phys 23:69–89. doi:10.1103/RevModPhys.23.69

Sadeghipour M, Terreux R, Phipps J (2005) Flavonoids and tyrosine nitration: structure–activity relationship correlation with enthalpy of formation. Toxicol In Vitro 19:155–165. doi:10.1016/j.tiv.2004.06.009

Sawa T, Ohshima H (2006) Nitrative DNA damage in inflammation and its possible role in carcinogenesis. Nitric Oxide 14:91–100. doi:10.1016/j.niox.2005.06.005

Scott AP, Radom L (1996) Harmonic vibrational frequencies: an evaluation of Hartree-Fock, Moller-Plesset, quadratic configuration interaction, density functional theory, and semiempirical scale factors. J Phys Chem 100:16502–16513. doi:10.1021/jp960976r

Stewart JJP (1989) Optimization of parameters for semiempirical methods. I. Method. J Comput Chem Soc 10:209–220. doi:10.1002/jcc.540100208

Stewart JJP (1990) MOPAC: a semiempirical molecular orbital program. J Comput Aided Mol Des 4:1–105. doi:10.1007/BF00128336

Trostchansky A, Rubbo H (2008) Nitrated fatty acids: mechanisms of formation, chemical characterization, and biological properties. Free Radic Biol Med 44:1887–1896. doi:10.1016/j.freeradbiomed.2008.03.006

URL1 (2008) http://www.sigmaaldrich.com/spectra/ftir/FTIR006921.PDF. Accessed 30 June 2008

Yermilov V, Rubio J, Ohshima H (1995a) Formation of 8-nitroguanine in DNA treated with peroxynitrite in vitro and its rapid removal from DNA by depurination. FEBS Lett 376:207–210. doi:10.1016/0014-5793(95)01281-6

Yermilov V, Rubio J, Becchi M, Friesen MD, Pignatelli B, Ohshima H (1995b) Formation of 8-nitroguanine by the reaction of guanine with peroxynitrite in vitro. Carcinogenesis 16:2045–2050. doi:10.1093/carcin/16.9.2045